South African National Space Agency - SANSA, Hermanus, 7 November 2013

Modelling solitary waves and shocks in suprathermal plasmas from first principles

Ioannis Kourakis (*)
Centre for Plasma Physics, Queen's University Belfast
Northern Ireland, UK

(*) Work carried out in collaboration with:
Gina Williams, Femi Adeyemi, Gareth Hefferon, Divya Sharma (Belfast, UK),
Manfred Hellberg (UKZN, Durban, S Africa), Sebastien Guisset (France)
Thomas Baluku (Uganda), Sharmin Sultana & Gaji Anowar (Dhaka, Bangladesh), Mehdi Jenab (
Ashkbiz Danehkar (Sydney, Australia), Nareshpal Singh Saini (GNDU India).

Special thanks: Frank Verheest (Gent, Belgium), Mark Dieckmann (Sweden)
Shimul Maharaj (SANSA, Hermanus SA)

Queen's University Belfast

Acknowledgments: NITheP, SANSA South Africa; UK EPSRC; UK Royal Society.

Layout

- 1. Motivation: Suprathermal electrons – occurrence, observations
- 2. Fundamental framework for superthermal plasmas:
  kappa (κ) distribution function, observation, phenomenology, earlier results
- 3. Effect on ES waves: linear and on solitary waves
- 4. Nonlinear self-modulation of ES wavepackets
  modulational instability & envelope solitons
- 5. Discussion, perspectives for further study
- 6. Conclusions

1. Motivation: superthermal distributions are ubiquitous

- Accelerated electron populations are tacitly detected in Space observations:
  Montgomery *et al*, PRL (1965), Vasyliunas, JGR (1968),
  Fitzenreiter *et al,* GRL (1998)
- Space plasmas: Saturn's Magnetosphere: Schippers *et al.* JGR 2008,
  Solar wind: Gaelzer & Yoon ApJ 2008; Gaelzer JGR 2010;
  Livadiotis & McComas JGR 2011
- Plasma laboratory experiments:
  Kharchenko *et al,* Nucl. Fusion (1961), Kardfidov *et al,* Sov. Phys. JETP (1990), S. Magni *et al,* PRE (2005), G Sarri *et al* PRL (2009)
- Numerical simulations:
  Petkaki J. Geophys. Res. (2003), Yoon *et al* PRL (2005), Kawahara *et al* JPSJ (2006), Lu *et al* J. Geophys. Res. (2010), Koen *et al* PoP (2012)
- Beam-plasma interactions, e-acceleration in a turbulent medium
  Yoon et al, PRL (2005)

+ Intense laser-matter interactions: M. Nakatsutsumi *et al*, NJP (2008);
  G Sarri *et al* (2010); experiments by Marco Borghesi and coll. @QUB Belfast.

2. κ (kappa) distribution - basics

$$f_\kappa(v) = \frac{n_0}{(\pi\kappa\theta^2)^{3/2}} \frac{\Gamma(\kappa+1)}{\Gamma(\kappa-1/2)} \left(1+\frac{v^2}{\kappa\theta^2}\right)^{-\kappa-1}$$

[Ref. Vasyliunas JGR (1968), ...,
Hellberg *et al*, PoP (2009)]

Effective thermal speed:

$$\theta^2 = \frac{\kappa-3/2}{\kappa}\left(\frac{2k_BT}{m}\right)$$

T : kinetic temperature

κ : spectral index

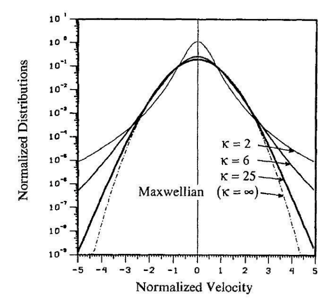

FIG. 1. Comparison of generalized Lorentzian distributions for the spectral index $\kappa = 2$, 6, and 25, with the corresponding Maxwellian distribution ($\kappa = \infty$).

[Figure from: Summers & Thorne, PF (1991)]

Kappa (κ) parameter measures deviation from thermal equilibrium:
Smaller κ value (1.5 < κ < 6) → long superthermal df tail, harder spectrum
Infinite κ value (κ > 10 approx.) → Maxwellian *df, no* superthermal particles

Kappa distribution function *(continued)*

- First introduced to fit early Space observations [Vasyliunas, PF 1968], suggesting superthermal electrons + *power-law dependence* in *v*
  [Montgomery *et al*, PRL 1965]
- Kappa distribution studied in linear regime: *modified Z_κ dispersion function* [Summers & Thorne, PF (1991), Mace & Hellberg PoP (1995, 2009)]
- Anomalous Landau damping of ES plasma modes
  [Podesta PoP (2005); Lee PoP (2007)]
- Satellite observations; Foreshock, Magnetotail, Plasma sheet; Solar Exosphere, Solar wind, Heliosheath … *(see next slides)*
- Solar Corona anomalous temperature variation explained via kappa theory [Scudder ApJ (1992), Maksimovic *et al*, A&A (1997)]
- Cassini data, Saturn: s/thermal cold/hot *e* obs. [Schippers *et al* JGR (2008)]

JOURNAL OF GEOPHYSICAL RESEARCH, VOL. 113, A07208, doi:10.1029/2008JA013098, 2008

Click Here for Full Article

Multi-instrument analysis of electron populations in Saturn's magnetosphere

P. Schippers,[1] M. Blanc,[1] N. André,[2] I. Dandouras,[1] G. R. Lewis,[3] L. K. Gilbert,[3] A. M. Persoon,[4] N. Krupp,[5] D. A. Gurnett,[4] A. J. Coates,[3] S. M. Krimigis,[6] D. T. Young,[7] and M. K. Dougherty[8]

Received 15 February 2008; revised 2 May 2008; accepted 7 May 2008; published 18 July 2008.

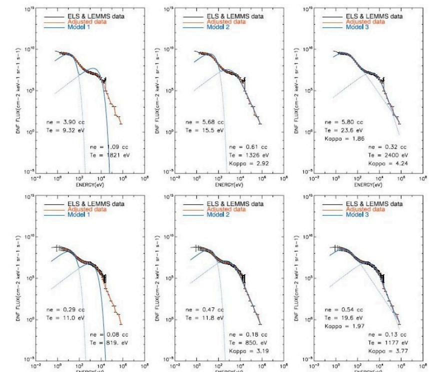

Figure 2. Composite CAPS/ELS and MIMI/LEMMS (energy channels C0-C7) spectral plots of electron intensities versus energy, observed at (top) 2200 UT (R = 9 R_s, local time 18.32 h, latitude 0.23 degrees) and at (bottom) 0727 UT (R = 12.8 R_s, local time 19.82 h, latitude 0.35 degrees) on days of year 142 and 143 of 2006 during Rev. 24, respectively. Original data are represented in black, our interpolated data are represented in red, and the results of our various models are represented in blue. (left) Model with 2 Maxwellian distributions. (middle) Model with one Maxwellian and one kappa distribution. (right) Model with two kappa distributions.

Cassini data from Saturn;
from:
Schippers *et al* JGR (2008)
Excellent 2-kappa df fit
over regions
$5.4\,R_S < R < 18\,R_S$

JOURNAL OF GEOPHYSICAL RESEARCH, VOL. 116, A04227, doi:10.1029/2010JA016112, 2011

Electron acoustic waves in double-kappa plasmas: Application to Saturn's magnetosphere

T. K. Baluku,[1,2] M. A. Hellberg,[1] and R. L. Mace[1]

Received 11 September 2010; revised 30 December 2010; accepted 11 February 2011; published 23 April 2011.

[1] Using a kinetic theoretical approach, the characteristics of electron acoustic waves (EAWs) are investigated in plasmas whose electron velocity distributions are modeled by a combination of two kappa distributions, with distinct densities, temperatures, and κ values. The model is applied to Saturn's magnetosphere, where the electrons are well fitted by such a double-kappa distribution. The results of this model suggest that EAWs will be weakly damped in regions where the hot and cool electron densities are approximately equal, the hot to cool temperature ratio is about 100, and the kappa indices are roughly constant, with $\kappa_c \simeq 2$ and $\kappa_h \simeq 4$, as found in Saturn's outer magnetosphere ($R \sim 13$ 18 R_S, where R_S is the radius of Saturn). In the inner magnetosphere ($R < 9\ R_S$), the model predicts strong damping of EAWs. In the intermediate region (9 13 R_S), the EAWs couple to the electron plasma waves and are weakly damped.

Citation: Baluku, T. K., M. A. Hellberg, and R. L. Mace (2011), Electron acoustic waves in double-kappa plasmas: Application to Saturn's magnetosphere, *J. Geophys. Res.*, *116*, A04227, doi:10.1029/2010JA016112.

PHYSICS OF PLASMAS **19**, 042102 (2012)

A simulation approach of high-frequency electrostatic waves found in Saturn's magnetosphere

Etienne J. Koen,[1,2,a)] Andrew B. Collier,[1,3,b)] and Shimul K. Maharaj[1]
[1]*South African National Space Agency (SANSA), Space Science, Hermanus, South Africa*
[2]*Royal Institute of Technology (KTH), Stockholm, Sweden*
[3]*University of KwaZulu-Natal, Durban, South Africa*

(Received 3 December 2011; accepted 29 February 2012; published online 5 April 2012)

Using a particle-in-cell simulation, the characteristics of electron plasma and electron acoustic waves are investigated in plasmas containing an ion and two electron components. The electron velocities are modeled by a combination of two κ distributions. The model applies to the extended plasma sheet region in Saturn's magnetosphere where the cool and hot electron velocities are found to have low indices, $\kappa_c \simeq 2$ and $\kappa_h \simeq 4$. For such low values of κ_c and κ_h, the electron plasma and electron acoustic waves are coupled. The model predicts weakly damped electron plasma waves while electron acoustic waves should also be observable, although less prominent. [http://dx.doi.org/10.1063/1.3695404]

JOURNAL OF GEOPHYSICAL RESEARCH, VOL. 115, A09109, doi:10.1029/2009JA015217, 2010

Effect of superthermal electrons on Alfvén wave propagation in the dusty plasmas of solar and stellar winds

R. Gaelzer,[1] M. C. de Juli,[2] and L. F. Ziebell[3]

Received 21 December 2009; revised 25 April 2010; accepted 26 May 2010; published 22 September 2010.

[1] The dispersive characteristics and absorption coefficient of Alfvén waves propagating parallel to the ambient magnetic field are discussed, taking into account the effects of both the charged dust particles present in the interplanetary medium and the superthermal character of the electron distribution function, using physical parameters relevant for solar and stellar winds. The solar wind electrons are described by an isotropic κ distribution and the protons are described by a Maxwellian. The results are valid for a frequency regime well above the dust-plasma and dust-cyclotron frequencies. However, the theoretical formulation is fully kinetic and the dust charge variation is taken into account. The charging process of the dust is assumed to be associated with the capture of electrons and ions by the dust particles during inelastic collisions with the plasma particles. The dispersion relation for parallel-propagating Alfvén waves is numerically solved and the solutions are compared with particular situations where either the dust particles are absent or the electrons are described by a Maxwellian. It is shown that the presence of both the charged dust particles and the superthermal character of the electron distribution function sensibly modify the dispersion relation of low-frequency and long-wavelength Alfvén waves and significantly increase the absorption coefficient, strongly suggesting that both effects are equally important for a realistic description of the physical processes that occur in solar and stellar winds and that are influenced by the Alfvén waves, such as the energization of particles and the turbulent cascade of magnetic fluctuations.

Citation: Gaelzer, R., M. C. de Juli, and L. F. Ziebell (2010), Effect of superthermal electrons on Alfvén wave propagation in the dusty plasmas of solar and stellar winds, *J. Geophys. Res.*, *115*, A09109, doi:10.1029/2009JA015217.

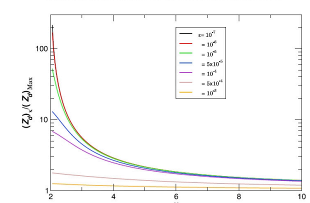

2. Ratio $(Z_d)_\kappa/(Z_d)_{\max}$ as a function of κ for different dust-particle concentrations (ϵ).

"Therefore, one can safely conclude that near the Sun, at 0.3 AU, the ratio is around 10, and at near-Earth distances, where kappa~5, the ratio is around 2. For kappa→10 the ratio approaches 1, as expected, because for large kappa the superthermal distribution approaches the Maxwellian. As the particle radius grows from 10−7 cm to 10−2 cm, which are typical dust sizes observed in the interplanetary environment [Mann, 2008], the surplus of electric charge on the dust due to the superthermal electrons becomes less pronounced. Moreover, this effect is expected to be more important for distances r near 1 AU, because this region is where the smaller values of kappa are observed [Štverák et al., 2009]."

Kinetic simulations of beam-plasma interactions (Yoon *et al* PRL, 2005)

PRL 95, 215003 (2005) PHYSICAL REVIEW LETTERS week ending 18 NOVEMBER 2005

Self-Consistent Generation of Superthermal Electrons by Beam-Plasma Interaction

Peter H. Yoon
Institute for Physical Science and Technology, University of Maryland, College Park, Maryland 20742, USA

Tongnyeol Rhee and Chang-Mo Ryu
Pohang University of Science and Technology (POSTECH), Pohang, Korea
(Received 11 July 2005; published 16 November 2005)

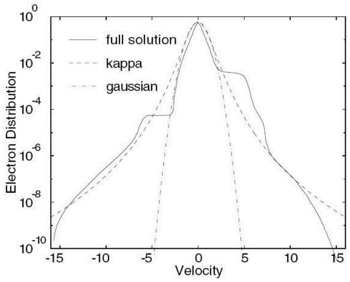

FIG. 4. Comparison of $F(u)$ at $\omega_{pe}t = 2 \times 10^4$ computed for $g = 5 \times 10^{-3}$ with κ distribution with index $\kappa = 3.5$ and the Gaussian.

PRL 99, 145002 (2007) PHYSICAL REVIEW LETTERS week ending 5 OCTOBER 2007

Theory of Weak Bipolar Fields and Electron Holes with Applications to Space Plasmas

Martin V. Goldman,[1] David L. Newman,[1] and André Mangeney[2]
[1]*Department of Physics and CIPS, University of Colorado, Boulder, Colorado 80309, USA*
[2]*DESPA, Observatoire de Meudon, Paris, France*
(Received 4 May 2007; published 5 October 2007)

A theoretical model of weak electron phase-space holes is used to interpret bipolar field structures observed in space. In the limit $e\phi_{max}/T_e \ll 1$ the potential of the structure has the unique form, $\phi(x) = \phi_{max}\mathrm{sech}^4(x/\alpha)$, where ϕ_{max} depends on the derivative of the trapped distribution at the separatrix, while α depends only on a screening integral over the untrapped distribution. Idealized trapped and passing electron distributions are *inferred* from the speed, amplitude, and shape of satellite waveform measurements of weak bipolar field structures.

DOI: 10.1103/PhysRevLett.99.145002 PACS numbers: 52.35.Sb, 52.35.Mw, 94.05.Fg

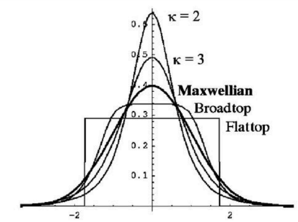

FIG. 1. Untrapped electron distributions used in Table I.

Electron-hole experiment: excellent fit for kappa < 4 ;

Cf. recent experiment by G Sarri *et al PoP* (2010) (see *next slide*)

PHYSICS OF PLASMAS 17, 010701 (2010)

Observation and characterization of laser-driven phase space electron holes

G. Sarri,[1] M. E. Dieckmann,[2] C. R. D. Brown,[3] C. A. Cecchetti,[1] D. J. Hoarty,[3] S. F. James,[3] R. Jung,[4] I. Kourakis,[1] H. Schamel,[5] O. Willi,[4] and M. Borghesi[1]
[1]*School of Mathematics and Physics, The Queen's University of Belfast, Belfast BT7 1NN, United Kingdom*
[2]*ITN, Linkoping University, 60174 Norrkoping, Sweden*
[3]*AWE, Aldermaston, Reading, Berkshire RG7 4PR, United Kingdom*
[4]*Institute for Laser and Plasma Physics, Heinrich-Heine-University, 40225 Düsseldorf, Germany*
[5]*Physikalisches Institut, Universität Bayreuth, D-95440 Bayreuth, Germany*

(Received 12 November 2009; accepted 15 December 2009; published online 7 January 2010)

The direct observation and full characterization of a phase space electron hole (EH) generated during laser-matter interaction is presented. This structure, propagating in a tenuous, nonmagnetized plasma, has been detected via proton radiography during the irradiation with a ns laser pulse ($I\lambda^2 \approx 10^{14}$ W/cm^2) of a gold *hohlraum*. This technique has allowed the simultaneous detection of propagation velocity, potential, and electron density spatial profile across the EH with fine spatial and temporal resolution allowing a detailed comparison with theoretical and numerical models.

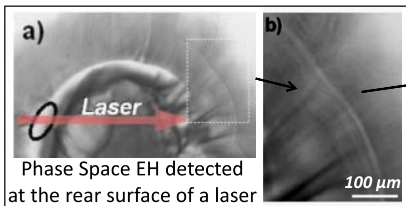

Phase Space EH detected at the rear surface of a laser irradiated target

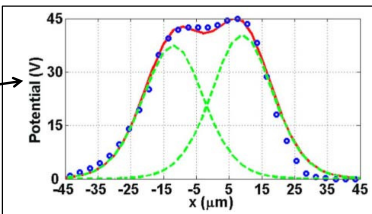

Potential profile fitted with two bell-shaped, κ-dependent soliton curves:

$$\phi(x) = \phi_{max}\,\mathrm{sech}^4\left(\frac{x}{4\sqrt{\gamma_e}}\right)$$

κ-dependent parameter: $\kappa \sim 4$

- Incomplete thermalization of the background plasma
- Hot electron population accelerated by the laser

↓

Fit by κ-distributed plasma electron distribution

PHYSICS OF PLASMAS 17, 082305 (2010)

Shock creation and particle acceleration driven by plasma expansion into a rarefied medium

G. Sarri,[1] M. E. Dieckmann,[2] I. Kourakis,[1] and M. Borghesi[1]
[1]*Centre for Plasma Physics, The Queen's University of Belfast, Belfast BT7 1NN, United Kingdom*
[2]*VITA ITN, Linkoping University, 60174 Norrkoping, Sweden*

(Received 26 March 2010; accepted 6 July 2010; published online 19 August 2010)

The expansion of a dense plasma through a more rarefied ionized medium is a phenomenon of interest in various physics environments ranging from astrophysics to high energy density laser-matter laboratory experiments. Here this situation is modeled via a one-dimensional particle-in-cell simulation; a jump in the plasma density of a factor of 100 is introduced in the middle of an otherwise equally dense electron-proton plasma with an uniform proton and electron temperature of 10 eV and 1 keV, respectively. The diffusion of the dense plasma, through the rarefied one, triggers the onset of different nonlinear phenomena such as a strong ion-acoustic shock wave and a rarefaction wave. Secondary structures are detected, some of which are driven by a drift instability of the rarefaction wave. Efficient proton acceleration occurs ahead of the shock, bringing the maximum proton velocity up to 60 times the initial ion thermal speed. © 2010 American

Non-Maxwellian behaviour of the electron density distribution of a plasma expanding into a rarefied medium has been seen in PIC sims

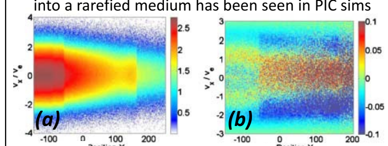

(a) Phase space of the expanding electrons.
(b) Electron distribution function normalised to a Maxwellian with same density and temperature.

Non-thermality generated by the counterstreaming electrons of the rarefied medium.
Suppression of Weibel instability → electrostatic plasma evolution

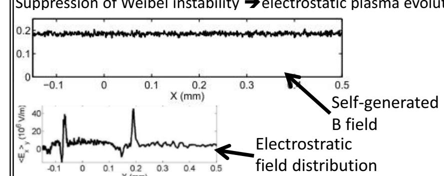

Clear difference from expansion into vacuum!

Kappa df *versus* Tsallis theory

- Apparent relation suggested between kappa *df* and *q-Gaussian df* emerging as a generic configuration within the *nonextensive (Tsallis) thermodynamics* framework [Tsallis J Stat Phys 1988];
- Rigorous link unclear, yet recent study claims equivalence proven [Milovanov 2000; Livadiotis & McComas JGR 2009, ApJ 2010, SSR 2013]
- Dedicated Special Session @AGU Fall meeting, San Francisco Dec.'13

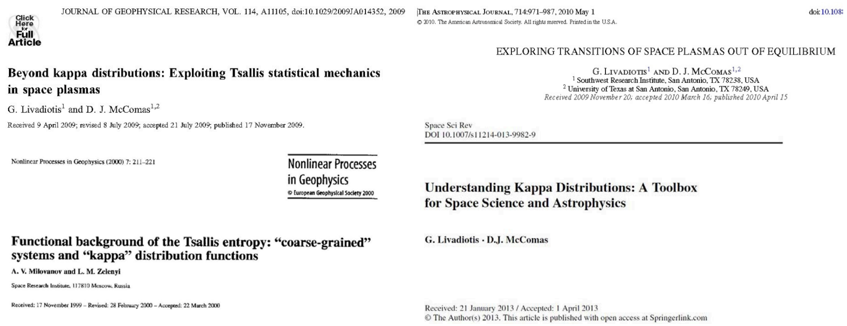
JOURNAL OF GEOPHYSICAL RESEARCH, VOL. 114, A11105, doi:10.1029/2009JA014352, 2009

Beyond kappa distributions: Exploiting Tsallis statistical mechanics in space plasmas

G. Livadiotis[1] and D. J. McComas[1,2]

Received 9 April 2009; revised 8 July 2009; accepted 21 July 2009; published 17 November 2009.

Nonlinear Processes in Geophysics (2000) 7: 211–221

Nonlinear Processes in Geophysics © European Geophysical Society 2000

Functional background of the Tsallis entropy: "coarse-grained" systems and "kappa" distribution functions

A. V. Milovanov and L. M. Zelenyi

Space Research Institute, 117810 Moscow, Russia

Received: 17 November 1999 – Revised: 28 February 2000 – Accepted: 22 March 2000

THE ASTROPHYSICAL JOURNAL, 714:971–987, 2010 May 1

© 2010. The American Astronomical Society. All rights reserved. Printed in the U.S.A.

EXPLORING TRANSITIONS OF SPACE PLASMAS OUT OF EQUILIBRIUM

G. LIVADIOTIS[1] AND D. J. MCCOMAS[1,2]

[1] Southwest Research Institute, San Antonio, TX 78238, USA

[2] University of Texas at San Antonio, San Antonio, TX 78249, USA

Received 2009 November 20; accepted 2010 March 16; published 2010 April 15

Space Sci Rev
DOI 10.1007/s11214-013-9982-9

Understanding Kappa Distributions: A Toolbox for Space Science and Astrophysics

G. Livadiotis · D.J. McComas

Received: 21 January 2013 / Accepted: 1 April 2013

© The Author(s) 2013. This article is published with open access at Springerlink.com

Space Sci Rev
DOI 10.1007/s11214-013-9982-9

Understanding Kappa Distributions: A Toolbox for Space Science and Astrophysics

G. Livadiotis · D.J. McComas

Understanding Kappa Distributions: A Toolbox for Space Science

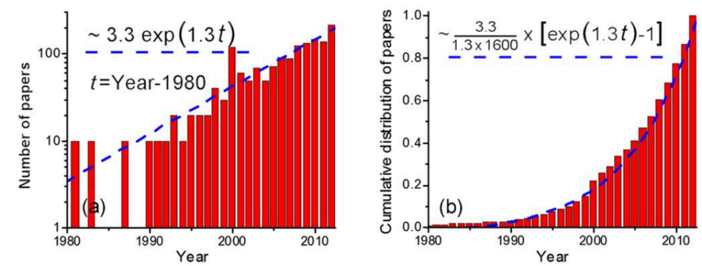

Fig. 1 (**a**) Number and (**b**) cumulative distribution of $N \sim 1600$ papers cataloged in Google Scholar from 1980 through 2012 that are related to kappa distributions and include these distributions in their title. The fit curve (*blue dash*) in both panels show the exponential growth of these studies

3. Dust-ion acoustic solitary waves

(cold fluid "toy-model" + kappa-distributed electrons)

Continuity: $$\frac{\partial n}{\partial t} + \frac{\partial (n u)}{\partial x} = 0$$

Momentum: $$\frac{\partial u}{\partial t} + u\frac{\partial u}{\partial x} = -\frac{\partial \phi}{\partial x}$$

Poisson Eq.: $$\frac{\partial^2 \phi}{\partial x^2} = -n + n_e \mp Z_d n_d$$

dust (immobile)

S/thermal electrons: $$n_e = n_{e,0}\left(1 - \frac{\phi}{\kappa - 3/2}\right)^{-\kappa+1/2}$$

Scaling: $n = \frac{n_i}{n_{i0}}$, $u = \frac{u_i}{c_s}$, $x = \frac{x}{\lambda_D}$, $\phi = \frac{e\phi}{k_B T_e}$, $t = \omega_{pi} t$

$$c_s = \left(\frac{k_B T_e}{m_i}\right)^{1/2} \qquad \omega_{pi} = \left(\frac{4\pi n_{i0} e^2}{m_i}\right)^{1/2} \qquad \lambda_D = \left(\frac{k_B T_e}{4\pi n_{i0} e^2}\right)^{1/2}$$

[* in collaboration with: NS Saini, S Sultana, T Baluku, M Hellberg]

Pseudopotential formalism for IA travelling waves

[Vedenov & Sagdeev 1961, Sagdeev 1966, Verheest & Hellberg 2009 (review, Nova publ.)]

- stationary frame, single travelling coordinate $\xi = x - Mt$

* reduction of the fluid model PDEs in *{x, t}* to an ODE in ξ

* pseudo-energy-balance equation:

$$\frac{1}{2}\left(\frac{d\phi}{d\xi}\right)^2 + V(\phi) = 0$$

$$V(\phi) = M^2\left(1 - \sqrt{1 - \frac{2\phi}{M^2}}\right) + 1 - \left(1 - \frac{\phi}{\kappa - 3/2}\right)^{-\kappa+3/2}$$

* solution obtained (numerically) for the electric potential ϕ

* density and fluid velocity given by

$$n = \frac{1}{\sqrt{1 - 2\phi/V^2}} \qquad v = V - \sqrt{V^2 - 2\phi}$$

The generic solitary wave (pulse) solution bears the form:

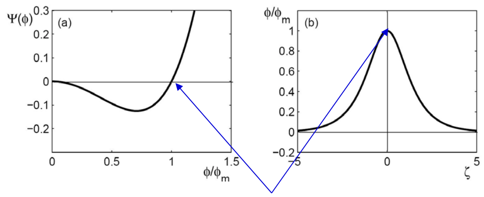

potential pulse amplitude = root of V

Slower "supersonic" (but not subsonic!) solitons

for smaller kappa values:

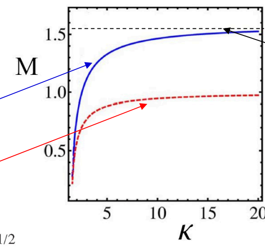

Known limit 1.58 for infinite κ

M_2: infinite compression point (choked flow)

M_1: κ-dependent "sound speed" $M_1 \equiv \left(\frac{\kappa - 3/2}{\kappa - 1/2} \right)^{1/2}$

FIG. 1. (Color online) IA soliton existence domain in the parameter space of κ and Mach number, M. Solitons may be supported in the region between the two curves. The lower, dashed curve represents the minimum (soliton) condition, M_1, and the upper, solid curve the infinite compression limit, M_2.

[* From: NS Saini, I Kourakis and M Hellberg, PoP **16**, 062903 (2009)]

Increased soliton amplitude for higher speed M (for given κ):

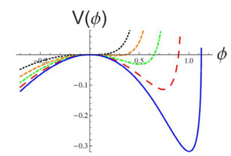

FIG. 2. (Color online) Variation of $V(\phi)$ for $\kappa=16$ and different values of Mach number, M. From top to bottom: Dotted curve: $M=0.97$; dashed curve: $M=1.10$; dotted-dashed curve: $M=1.23$; long-dashed curve: $M=1.36$; and solid curve: $M=1.50$.

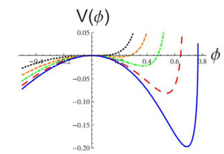

FIG. 3. (Color online) Variation of $V(\phi)$ for $\kappa=4$ and different values of Mach number, M. From top to bottom: Dotted curve: $M=0.85$; dashed curve: $M=0.95$; dotted-dashed curve: $M=1.05$; long-dashed curve: $M=1.15$; and solid curve: $M=1.24$.

and…

increased soliton amplitude for smaller kappa values (for fixed M) by a factor ~ 1.1 – 5: see bottom left

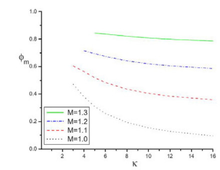

FIG. 8. (Color online) Variation of ϕ_m with κ for different values of the Mach number, M. The dotted curve corresponds to $M=1.0$; the dashed curve to $M=1.1$; the dotted-dashed curve to $M=1.2$; and the solid curve to $M=1.3$.

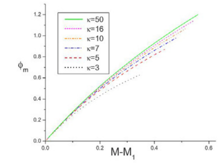

FIG. 4. (Color online) Variation of ϕ_m with $M-M_1$ for different values of κ. The dotted curve corresponds to $\kappa=3$, the dashed curve to $\kappa=5$, the dotted-dashed curve to $\kappa=7$, the dotted-dotted dashed curve to $\kappa=10$, the short-dashed curve to $\kappa=16$, and the solid curve to $\kappa=50$.

From: N S Saini, I Kourakis and MA Hellberg, Phys. Plasmas **16** 062903 (2009)

Increased soliton amplitude for lower κ !

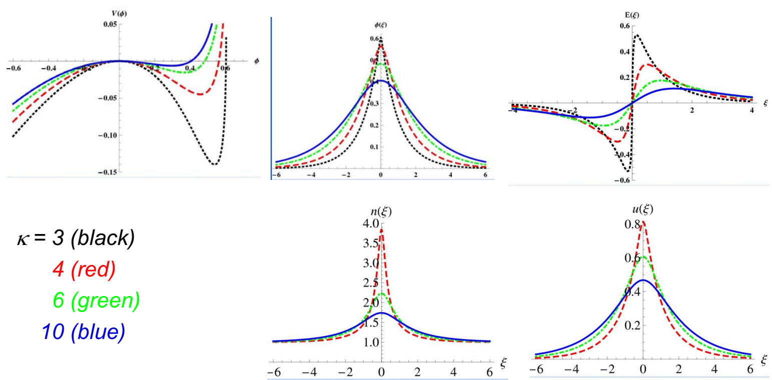

κ = 3 (black)

4 (red)

6 (green)

10 (blue)

- Strong dependence on κ in the range (3, 6);

- Quasi-Maxwellian behavior beyond *κ = 10.*

From: N S Saini, I Kourakis and MA Hellberg, Phys. Plasmas **16** 062903 (2009)

Analogous results obtained for obliquely propagating IA solitons in magnetized plasmas: increased soliton amplitude for lower κ

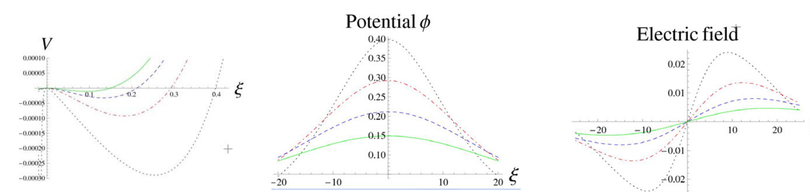

kappa = 3.5 (black); 5 (red); 7 (blue) ; 10 (green)

(and M=0.8, $\cos\theta$ =0.8, $\Omega^2 / \omega_p^2 = 0.02$)

From: S Sultana, I Kourakis, NS Saini and MA Hellberg, Phys. Plasmas **17** 032310 (2010)

DIA solitons (1): pseudopotential method

Soliton existence diagram, in terms of the dust parameter f :

- *cold ions+Maxwellian (left): immobile dust vs mobile dust*
- *cool ions+mobile dust (right): Maxwellian vs superthermal*

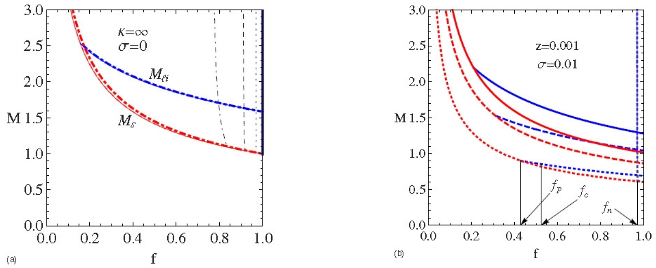

FIG. 2. (Color online) Existence domain for DIA solitons. Upper panel: Maxwellian electrons, cold ions ($\sigma=0$); immobile dust ($z=0$, continuous curves), as in Ref. 5; and mobile dust [$z=0.001$ (dotted curves), $z=0.01$ (dashed curves), $z=0.1$ (dot-dashed curves)]. Positive solitons have a lower cutoff at $f\approx 0.16$. Negative solitons have a z-dependent upper cutoff at $f=0.85-1$. Lower panel: cool ions ($\sigma=0.01$), mobile dust ($z=0.001$); continuous curves ($\kappa=\infty$), dotted curves ($\kappa=4$), dashed curves ($\kappa=2$), respectively. Positive solitons are bounded at low f while negative solitons have a κ-independent upper bound close to $f=1$. We also show the values f_p, f_c and f_n explicitly for $\kappa=2$.

dust parameter :

$$f = N_{e0}/N_{i0} = 1 + sZ_d N_{d0}/N_{i0}$$

From: T Baluku, MA Hellberg, I Kourakis and NS Saini, Phys. Plasmas **17** 053702 (2010).

DIA solitons (2): Korteweg-de Vries (KdV) vs mKdV description

- *Positive-negative (KdV) soliton shift for high (negative) dust concentration*
- *Strong dependence of the soliton amplitude on κ*
- *Negative (weak) and positive (large) pulse co-existence in the presence of negative dust (via Sagdeev nethod or mKdV theory *)*
- *(* The latter feature is absent in KdV theory)*

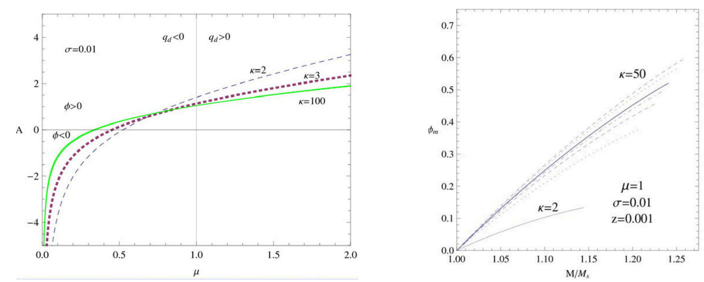

From: T Baluku, MA Hellberg, I Kourakis and NS Saini, Phys. Plasmas **17** 053702 (2010).

DIA solitons: the KdV paradigm

$$\frac{d\phi_1}{d\tau} + A\phi_1\frac{d\phi_1}{d\xi} + B\frac{d^3\phi_1}{d\xi^3} = 0\,, \tag{1}$$

for the potential disturbance ϕ_1. The nonlinearity (A) and dispersion (B) coefficients read

$$A = \frac{3\mu + \kappa(4-6\mu) - 4}{2\sqrt{(2\kappa-3)(2\kappa-1)(1-\mu)}}\,, \qquad B = \frac{1}{2}\left[\frac{(2\kappa-1)(1-\mu)}{2\kappa-3}\right]^{-3/2}\,, \tag{2}$$

or, in the Maxwellian electron limit ($\kappa\to\infty$), $A = \frac{2-3\mu}{2\sqrt{1-\mu}}$, $\quad B = \frac{1}{2}\left(\frac{1}{1-\mu}\right)^{3/2}$. In the dust-free limit (i.e. for $\mu = 0$), one recovers for ordinary ion-acoustic waves $A = \frac{2(\kappa-1)}{\sqrt{(2\kappa-3)(2\kappa-1)}}$, $\quad B = \frac{1}{2}\left(\frac{2\kappa-1}{2\kappa-3}\right)^{-3/2}$, which yields $A=1, B=1/2$ as expected [12] in the (dust-free) Maxwellian limit. The KdV equation (1) bears the soliton solution

$$\phi_1(\xi,\tau) = \phi_0\,\mathrm{sech}^2\left[(\xi - V\tau)/L_0\right]\,, \tag{3}$$

where the pulse amplitude ϕ_0 and the pulse width L_0, defined as $\phi_0 = 3V/A$ and $L_0 = \sqrt{4B/V}$ respectively satisfy the relation $\phi_0 L_0^2 = 12B/A$.

From: I Kourakis and S Sultana, AIP Conf Proceedings, **1397**, 86-91 (2011).

DIA solitons in action (1):

KdV soliton (propagating in Maxwellian plasma; κ=100, μ =0.1)

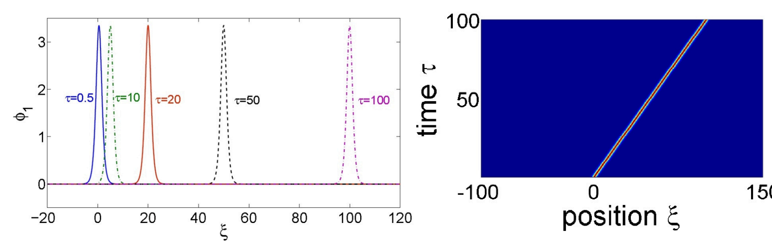

From: I Kourakis, S Sultana and MA Hellberg, Plasma Physics & Controlled Fusion (2012).

DIA solitons in action (1): high to low κ

KdV soliton (propagating in Maxwellian plasma; κ=100, μ =0.1)

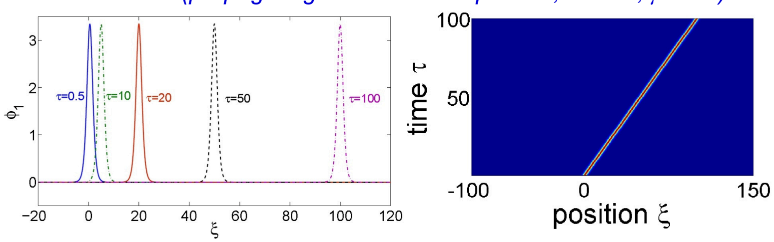

... enters a superthermal (κ=3) region:

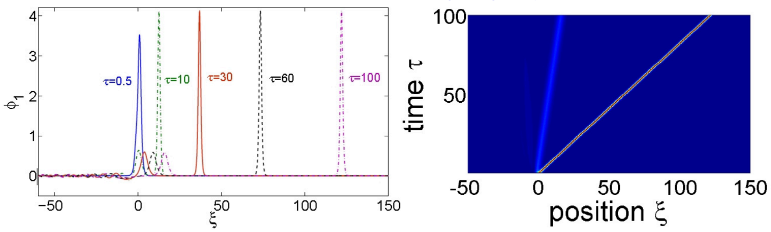

From: I Kourakis, S Sultana and MA Hellberg, Plasma Physics & Controlled Fusion (2012).

DIA solitons in action (2): low to high κ

KdV soliton (propagating in superthermal plasma; κ=3, μ =0.1)

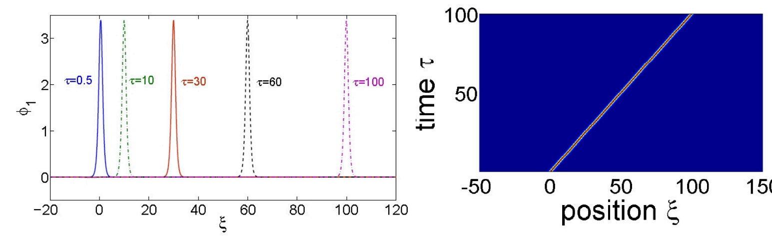

... enters a Maxwellian (κ=100) plasma region:

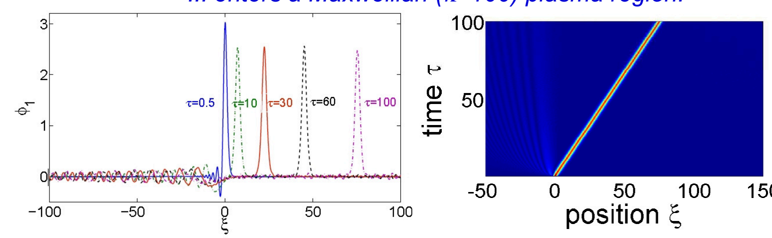

From: I Kourakis, S Sultana and MA Hellberg, Plasma Physics & Controlled Fusion (2012).

DIA solitons in action (3): dust effect

KdV soliton (propagating in superthermal plasma; κ=3, μ =0.1)

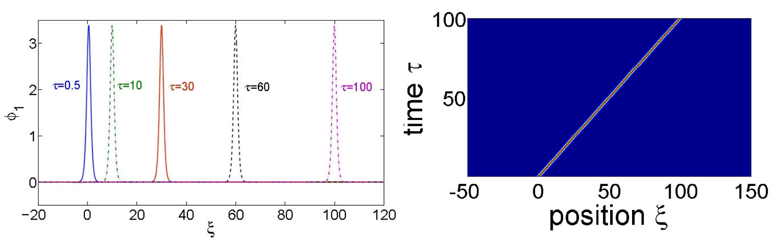

... enters a higher dust concentration (μ =0.3) plasma region:

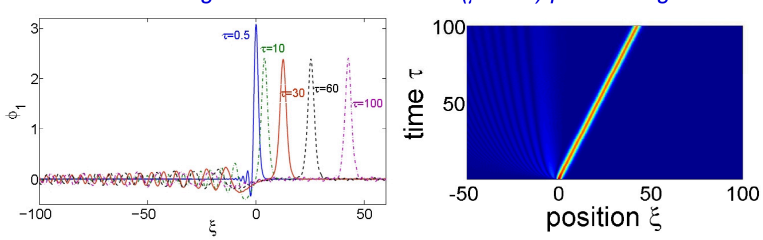

From: I Kourakis, S Sultana and MA Hellberg, Plasma Physics & Controlled Fusion (2012).

4. Nonlinear self-modulation of ES wavepackets *

- ***Amplitude modulation*** of ES plasma wavepackets due to carrier self-interaction: generic nonlinear mechanism, involving harmonic generation, modulational instability, envelope soliton generation, …

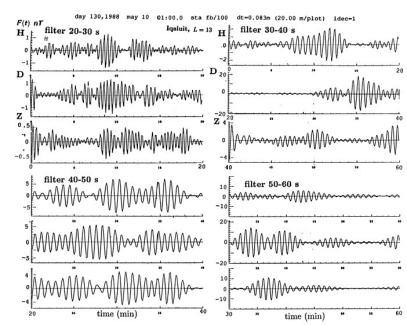

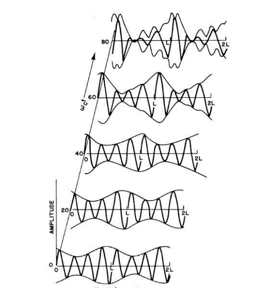

FIG. 1. Variation of wave amplitude A_y and energy $|A|$ with time and space; results of computer experiment.

[sources: Ya. Alpert, Phys. Reports **339**, 323 (2001)]); A Hasegawa PRL **24**, 1165 (1970)]

[* in collaboration with: S Sultana & NS Saini]

Background - literature

- On modulated ES waves: a Maxwellian background was considered for:
  - *Ion-acoustic waves (IAWs)*
    [Kakutani & Sugimoto, PF (1974), Durrani et al., PF (1979)]
  - Multi-ion plasma [Chabra & Sharma, PF (1986)]
  - Electron acoustic waves (EAWs) [Kourakis & Shukla, PRE (2004)]
  - Dusty plasmas: dust-ion-acoustic (DIA) & dust-acoustic (DA) modes
    [Kourakis & Shukla, PoP (2003); JPA (2003); Phys. Scr. (2004); NPG (2005)]

- Recent studies on ES wavepackets & amplitude modulation
  - in *kappa*-distributed plasmas:
  - DAWs [Saini & Kourakis, *Physics of Plasmas*, **15**, 123701 (2008)]
  - DIAWs [Sultana & Kourakis, in preparation]
  - EAWs [Sultana & Kourakis, *Plasma Phys. Cont. Fusion* **53** 045003 (2011)]
  - e-p plasmas: Esfandyari & I Kourakis, in preparation
  - \- in the *q-Tsallis* model:
  - IAWs [Bains *et al*, *Physics of Plasmas*, **18**, 022108 (2011)]

κ–dependent charge balance: expansion near equilibrium

- Normalized electron density:

$$\left(1-\frac{\phi}{\kappa-3/2}\right)^{-\kappa+1/2} \cong 1 + c_1\phi + c_2\phi^2 + c_3\phi^3 + \ldots$$

- Superthermality modeled via the κ–dependent coefficients:

$$c_1 = \mu\frac{2\kappa-1}{2\kappa-3}, \quad c_2 = \mu\frac{4\kappa^2-1}{2(2\kappa-3)^2}, \quad c_3 = \mu\frac{(4\kappa^2-1)(2\kappa+3)}{6(2\kappa-3)^3}$$

- Maxwellian *e-i* plasma limit (infinite κ): $c_n = 1/n! \quad (n = 1, 2, 3\ldots)$

- The *dust parameter* μ measures the dust concentration:

$$\mu = 1 + s\frac{Z_d n_d}{Z_i n_{i,0}}, \quad s = \pm 1$$ (for +/- dust charge sign)

i.e., $0 < \mu < 1$ for negative dust, while $\mu > 1$ for positive dust

Multiscale multiharmonic perturbation method

- Slow amplitude dynamics separated from fast carrier evolution

- State vector $S = (n, u, \phi)$ expanded near equilibrium $S^{(0)} = (1,0,0)$

$$S = S^{(0)} + \sum_{m=1}^{\infty} \varepsilon^m S^{(m)} \qquad m = 1, 2, 3\ldots\ldots$$

- Multi-harmonic expansion:

$$S^{(m)} = \sum_{l=-m}^{m} S_l^{(m)}(X_m, T_m)\ \exp[il(kx-\omega t)]$$

- Space/time variable stretching: $X_m = \varepsilon^m x, \quad T_m = \varepsilon^m t$

- Solution obtained to 2nd order (zeroth, 1st, 2nd harmonics):

$$S \cong \varepsilon S_1^{(1)} e^{i(kx-\omega t)} + \varepsilon^2 \left[S_2^{(0)} + S_2^{(2)} e^{2i(kx-\omega t)}\right] + O(\varepsilon^3)$$

Linear regime: modified dispersion properties

$$n_1^{(1)} = \left(k^2 + c_1\right)\phi_1^{(1)} \qquad u_1^{(1)} = \frac{k}{\omega}\phi_1^{(1)}$$

$$\omega^2 = \frac{k^2}{k^2 + c_1} \qquad c_1 = \frac{2\kappa-1}{2\kappa-3}$$

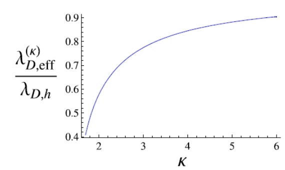

Figure 1. Variation of the electrostatic screening (effective Debye) length (scaled) with the superthermality parameter κ. See that the curve approaches unity at the infinite κ limit.

κ–modified Debye screening:
Shorter Debye length for small κ !

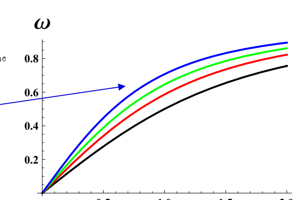

Blue: κ=∞ (Maxwellian)
Green: κ=4
Red: κ=2.6
Black: κ=2

(*) [Agreement with Bryant JPP (1996), Mace & Hellberg (PoP 1995)]

Dispersion relation: (a) dust *vs* (b) superthermality effect

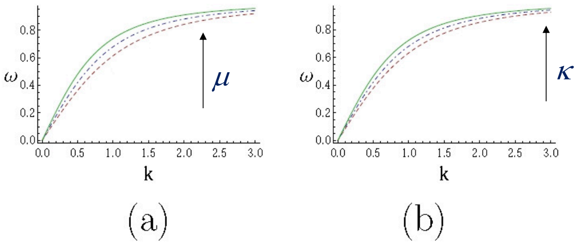

Figure 1: (Color online) Variation of the dust ion-acoustic wave frequency ω versus wavenumber k for (a) a different dust to ion number density μ, where $\mu = 0.01$ corresponds to dashed curve; $\mu = 0.3$ corresponds to dot-dashed curve; $\mu = 0.5$ corresponds to solid curve with superthermality index $\kappa = 3$ and (b) a different superthermality parameter κ, where $\kappa = 3$ corresponds to dashed curve; $\kappa = 5$ corresponds to dot-dashed curve; $\kappa = 100$ corresponds to solid curve with dust to ion number density $\mu = 0.1$.

From: S Sultana and I Kourakis, in preparation.

Group velocity: (a) dust *vs* (b) superthermality effect

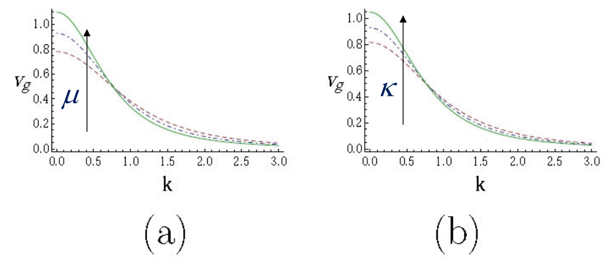

Figure 2: (Color online) Variation of the dust ion-acoustic group velocity v_g versus wavenumber k for (a) a different dust to ion number density μ, where $\mu = 0.01$ corresponds to dashed curve; $\mu = 0.3$ corresponds to dot-dashed curve; $\mu = 0.5$ corresponds to solid curve with superthermality index $\kappa = 3$ and (b) a different superthermality parameter κ, where $\kappa = 3$ corresponds to dashed curve; $\kappa = 5$ corresponds to dot-dashed curve; $\kappa = 100$ corresponds to solid curve with dust to ion number density $\mu = 0.1$.

From: S Sultana and I Kourakis, in preparation..

Non-linear Schrödinger Equation (NLSE)

Solution obtained to ~ε³ :

$$\phi \cong \varepsilon\, \psi\, e^{i(kx-\omega t)} + \varepsilon^2 \left[\phi_2^{(0)} + \phi_2^{(2)} e^{2i(kx-\omega t)}\right] + O(\varepsilon^3), \qquad \psi = \phi_1^1$$

The potential amplitude $\phi_1^{(1)} \equiv \psi(\zeta,\tau)$ satisfies:

$$i\frac{\partial\psi}{\partial\tau} + P\frac{\partial^2\psi}{\partial\zeta^2} + Q\,|\psi|^2\psi = 0$$

Slow envelope variables: $\zeta = \varepsilon(x - v_g t) \qquad \tau = \varepsilon^2 t$

Dispersion coefficient P: $P = -\frac{3c_1}{2}\frac{\omega^5}{k^4} = \frac{\omega''(k)}{2}$

Nonlinearity coefficient Q: $Q = \ldots = Q(k;\kappa;\ldots)$

Group velocity dispersion *P*: (a) dust *vs* (b) κ effect

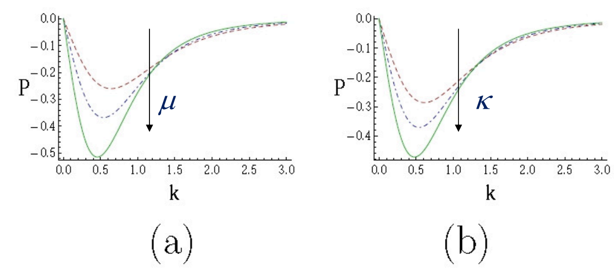

Figure 3: (Color online) Variation of the dispersion coefficient P of dust ion-acoustic wave versus wavenumber k for (a) a different dust to ion number density μ, where $\mu = 0.01$ corresponds to dashed curve; $\mu = 0.3$ corresponds to dot-dashed curve; $\mu = 0.5$ corresponds to solid curve with superthermality index $\kappa = 3$ and (b) a different superthermality parameter κ, where $\kappa = 3$ corresponds to dashed curve; $\kappa = 5$ corresponds to dot-dashed curve; $\kappa = 100$ corresponds to solid curve with dust to ion number density $\mu = 0.1$.

From: S Sultana and I Kourakis, in preparation.

Nonlinearity coefficient *Q*: (a) dust *vs* (b) κ effect

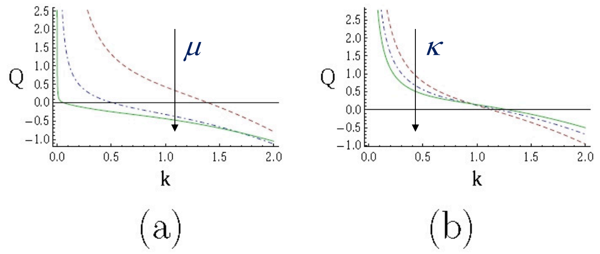

Figure 4: (Color online) Variation of the nonlinear coefficient Q of dust ion-acoustic wave versus wavenumber k for (a) a different dust to ion number density μ, where $\mu = 0.01$ corresponds to dashed curve; $\mu = 0.3$ corresponds to dot-dashed curve; $\mu = 0.5$ corresponds to solid curve with superthermality index $\kappa = 3$ and (b) a different superthermality parameter κ, where $\kappa = 3$ corresponds to dashed curve; $\kappa = 5$ corresponds to dot-dashed curve; $\kappa = 100$ corresponds to solid curve with dust to ion number density $\mu = 0.1$.

From: S Sultana and I Kourakis, in preparation.

Modulational (in)stability (MI) analysis

Nonlinear (amplitude perturbation) dispersion relation:

$$\hat{\omega}^2 = P\hat{k}^2\left(P\hat{k}^2 - 2Q|\hat{\psi}_{1,0}|^2\right)$$

For *P/Q* < *0*, a plane wave is modulationally stable;

For *P/Q* > *0*, a wavepacket is *unstable*; the *MI threshold* reads:

$$\hat{k} < k_{cr} \equiv \sqrt{\frac{2Q}{P}}\,|\hat{\psi}_{1,0}|$$

Maximum instability growth rate (κ dependent): $\Gamma_{\max} = Q\,|\hat{\psi}_{1,0}|^2$

Enhanced instability growth rate Γ due to superthermality:

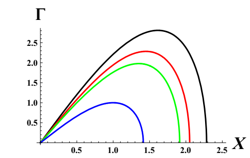

Black: κ=2.5
Red: κ=3
Green: κ=3.5
Blue: κ=∞ (Maxwellian)

Envelope (NLS) solitons

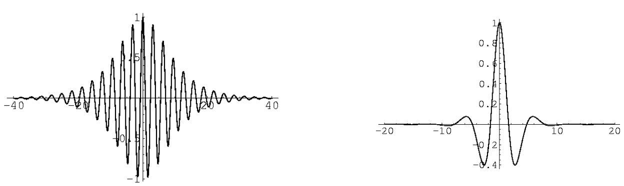

Bright-type envelope solitons (for P/Q>0)

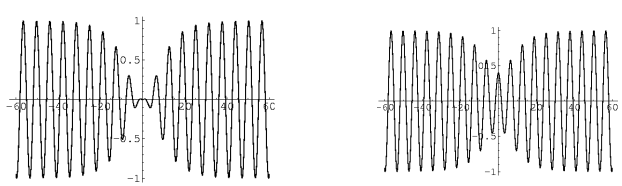

Dark (black/grey) type envelope solitons (for P/Q<0)

Modulational instability *live*

A monochromatic wavepacket breaks up, and may evolve into a series of localized pulses (envelope soliton train)

Plasma Phys. Control. Fusion **53** (2011) 045003 S Sultana and I Kourakis

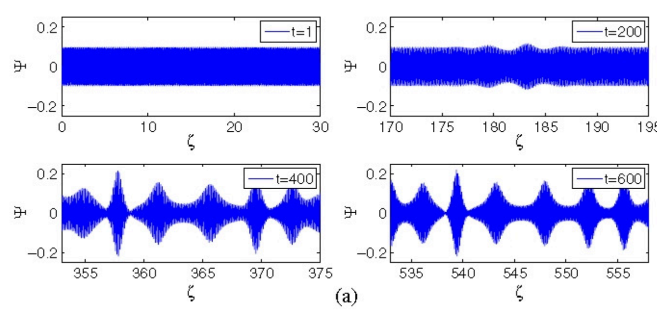

Parametric investigation of soliton characteristics (1)

$$L\psi_0 = (P/Q)^{1/2}$$

- *Superthermality leads to a decrease in envelope width L* (for given amplitude ψ): *enhanced envelope localization!*
- Lower instability threshold k_{cr} with smaller kappa
- Both effects intensified with negative dust (right frame: $\mu = 0.8$)

Lower instability threshold in the presence of dust !

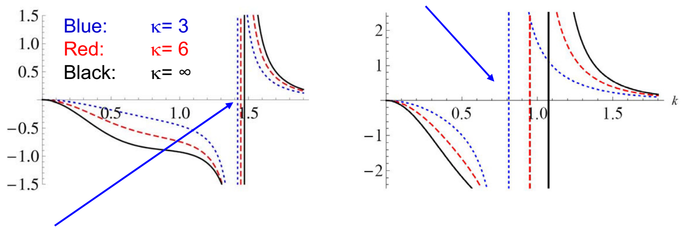

- *Agreement (k_{cr}= 1.47) with Kakutani & Sugimoto PF,1974 (Maxwellian e-i plasma)*

Parametric investigation of soliton characteristics (2)

- Modified instability threshold k_{cr} with kappa *and* with dust
- Modulational instability (MI) occurs at *longer wavelengths, in the presence of negative dust*
- MI less relevant with *positive dust*: stable wavepackets
- Remark: Landau damping omitted (yet less relevant for +d)

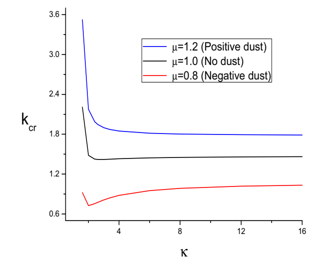

P/*Q ratio*: (a) dust *vs* (b) κ effect

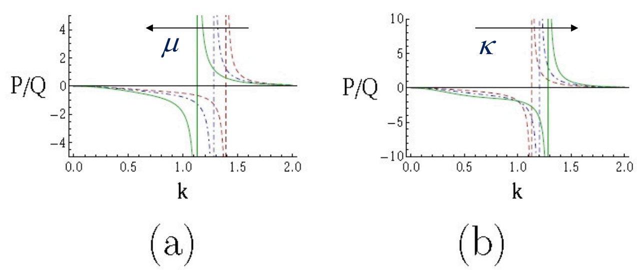

Figure 5: (Color online) Variation of P/Q versus wavenumber k for (a) a different dust to ion number density μ, where $\mu = 0.01$ corresponds to dashed curve; $\mu = 0.05$ corresponds to dot-dashed curve; $\mu = 0.1$ corresponds to solid curve with superthermality index $\kappa = 3$ and (b) a different superthermality parameter κ, where $\kappa = 3$ corresponds to dashed curve; $\kappa = 5$ corresponds to dot-dashed curve; $\kappa = 100$ corresponds to solid curve with dust to ion number density $\mu = 0.1$.

From: S Sultana and I Kourakis, in preparation .

Stability profile dependence on superthermality (κ) (for fixed *k*)

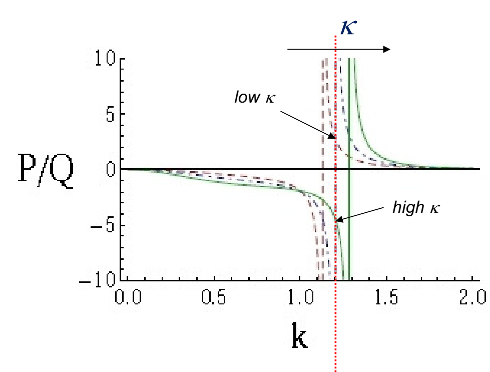

From: S Sultana and I Kourakis, in preparation..

DIA envelope solitons in action (1):

envelope solitons in superthermal plasma (κ=3, μ=0.1, k=1.2)

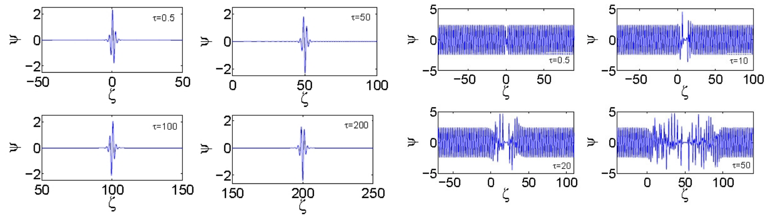

versus envelope solitons in Maxwellian plasma (κ=100, μ=0.1, k=1.2):

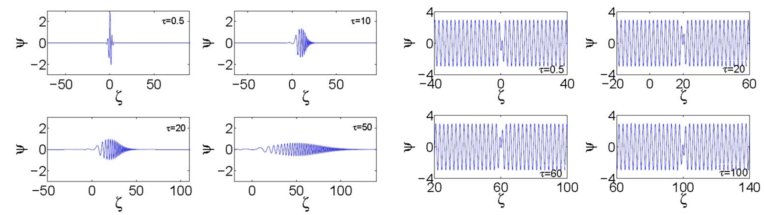

From: S Sultana and I Kourakis, in preparation.

DIA envelope solitons in action (2): superthermality effect

bright envelope solitons (k=1.2, μ=0.1): stable for κ=3, unstable for κ=100

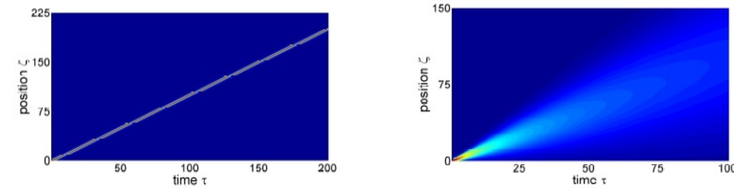

***dark** envelope solitons (k=1.2, μ=0.1): stable for κ=100, unstable for κ=3*

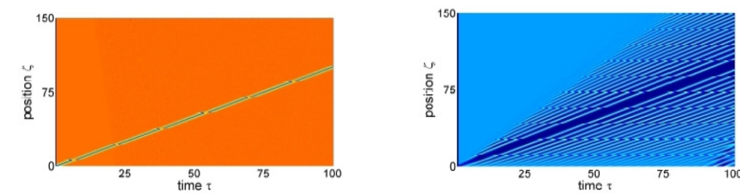

From: S Sultana and I Kourakis, in preparation.

Stability profile dependence on the dust concentration (μ) (for fixed *k*)

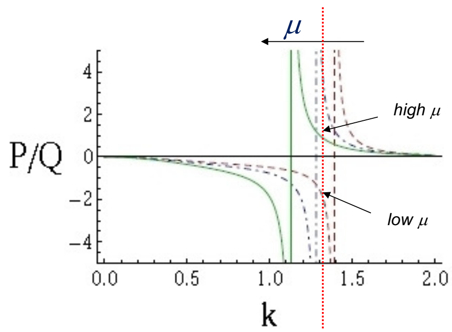

From: S Sultana and I Kourakis, in preparation.

DIA envelope solitons in action (3): dust concentration effect

bright envelope solitons (k=1.3, κ=3): stable for μ=0.1, unstable for μ=0.01

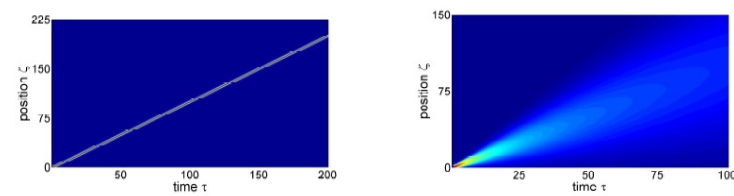

***dark** envelope solitons (k=1.3, κ=3): stable for μ=0.01, unstable for μ=0.1*

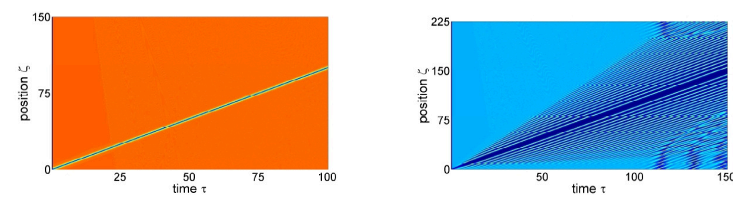

From: S Sultana and I Kourakis, in preparation.

Directions of further study & active investigations

- Dust acoustic waves: kappa effect on charging ; numerical study
- Electron acoustic waves: role of dust?
- Shocks in superthermal dusty plasmas
- Beam effects
- Particle trapping; BGK modes
- Detailed comparison with Space observations & experiments
- *Landau damping* effect: numerical study via Vlasov simulations
- Active collaboration (on the kappa project) with:
  MA Hellberg (S Africa), F Verheest (Belgium),
  T Baluku (Uganda), S Sultana & G Anowar (Bangladesh),
  NS Saini (India), A Danehkar (Australia), M Jenab (Iran).

Conclusions

- Accelerated electrons are present in most plasmas
- Superthermal plasmas are efficiently modelled by a *kappa df*
- Increased superthermality (smaller k) leads to:
  - A strong modification in the characteristics of ES solitary waves
  - Enhanced modulational instability
  - Stronger energy localization due to carrier self-modulation
- Results compatible with Space observations and experiments
- Minus: *Landau damping* neglected (fluid model).

Thanks:

Local team @QUB (present and ex):
Sharmin Sultana, Gianluca Sarri, Mehdi Jenab, Naresh Pal Singh Saini, Ashutosh Sharma, Ashkbiz Danehkar, Femi Adeyemi, Divya Sharma, Gareth Hefferon

Collaboration (kappa project) with:
Manfred Hellberg (UKZN, Durban, S Africa) & Thomas Baluku (Uganda)

Feedback from: G Livadiotis & DJ McComas (San Antonio, Texas USA)

***Special thanks** to:* Frank Verheest (U. Gent, Belgium),
Sergey Vladimirov (U. Sydney, Australia).
Padma Shukla (Bochum, Germany) (deceased, 2013)

Acknowledgements: support from: NITheP (SA), SANSA, UK EPSRC, UK Royal Society.

Material from:

NS Saini & I Kourakis, *Phys. Plasmas* **15** 123701 (2008)
NS Saini, I Kourakis and MA Hellberg, *Phys. Plasmas* **16** 062903 (2009)
MA Hellberg, TK Baluku, RL Mace, NS Saini and I. Kourakis, *Phys. Plasmas* **16** 094701 (2009)
TK Baluku, MA Hellberg, N S Saini & I Kourakis, Phys. Plasmas **17 053702** (2010)
S Sultana, I Kourakis, NS Saini, MA Hellberg, Phys. Plasmas **17** 032310 (2010)
S Sultana & I Kourakis, Plasma Phys. Controlled Fusion, **53** 045003 (2011).
I Kourakis, S Sultana & MA Hellberg, Plasma Phys. Controlled Fusion, **54** 124001 (2012).

www.kourakis.eu